41 総コレステロール(TC), LDL-コレステロール(LDL-C)

基準範囲

- 成人男性・女性　LDL-C：≦139 mg/dL[注1]
  (120～139 mg/dL の場合は，境界領域高 LDL-C 血症に分類される)

[参考下限値][注2]

- 成人男性・閉経前女性
  TC：133 mg/dL
  LDL-C：65 mg/dL
- 閉経後女性
  TC：152 mg/dL
  LDL-C：86 mg/dL

生理的変動

新生児では，TC は 65 mg/dL 程度，LDL-C は 25 mg/dL 程度である．生後 3～4 ヵ月後には，3 倍程度に上昇する．男性では，加齢に伴いゆっくりと上昇し，60 歳代以降に軽度低下する．女性では，閉経後に上昇し 50～60 歳代をピークとする．TC および LDL-C は，朝が最も高く日中わずかに低下するが，日内変動は通常考慮しなくてよい．リポ蛋白は原則として血管壁を自由には通過できないため，採血時の体位が違うと測定値が変動する[3]．変動幅の絶対値は，高コレステロール血症患者ほど大きいので注意が必要である．

検査の概要・臨床的意義

血中のコレステロールは，トリグリセリド(TG)とリン脂質とともに，蛋白と結合して複合体(リポ蛋白)を形成している．TC は，各リポ蛋白分画中のコレステロールの総和を表す．リポ蛋白は，カイロミクロン，超低比重リポ蛋白(VLDL)，低比重リポ蛋白(LDL)，高比重リポ蛋白(HDL)に分類される．TC の増加は，通常 LDL-C の増加を反映するが，高 HDL-C 血症でも TC は増加する．TC は酵素法で，LDL-C は計算法(Friedewald の式)[4]か LDL-C 直接法で測定する．

「動脈硬化性疾患予防ガイドライン 2012 年版」では，原則として 10～12 時間以上絶食後の空腹時に採血し，TG が 400 mg/dL 未満なら，計算式で LDL-C を求める(＝TC－TG/5－HDL コレステロール)よう求めている[1]．LDL-C の管理目標値は，図 2-12 に示すフローチャートを用いて 4 つのカテゴリー別に決定する．その際に，性別，年齢，喫煙の有無，収縮期血圧，TC 値を組み込んだチャートから求めた冠動脈疾患発症の絶対リスクを用いる．なお，食後検体や TG が 400 mg/dL 以上で計算式で LDL-C を求められない場合は，TC から HDL-C を引いた non HDL-C を管理目標値として用いる(表 2-14)．

高コレステロール(高 LDL-C)血症は，動脈硬化性疾患(特に虚血性心疾患と虚血性脳梗塞)のリスクを上昇させる．脂質低下剤により LDL-C を下げれば，虚血性心疾患の発症リスクは 20～30％低下する．一方，低コレ

注 1：「動脈硬化性疾患予防ガイドライン 2012 年版」[1]で設定されている病態識別値である．TC は，2002 年版のガイドラインまで高コレステロール血症の診断基準(220 mg/dL 以上)に用いられていたが，2007 年版より除かれた．
注 2：健常人の 5 パーセンタイルに相当する値(約 2,500 名の健診受診者および健常ボランティアのデータより算出)[2]．

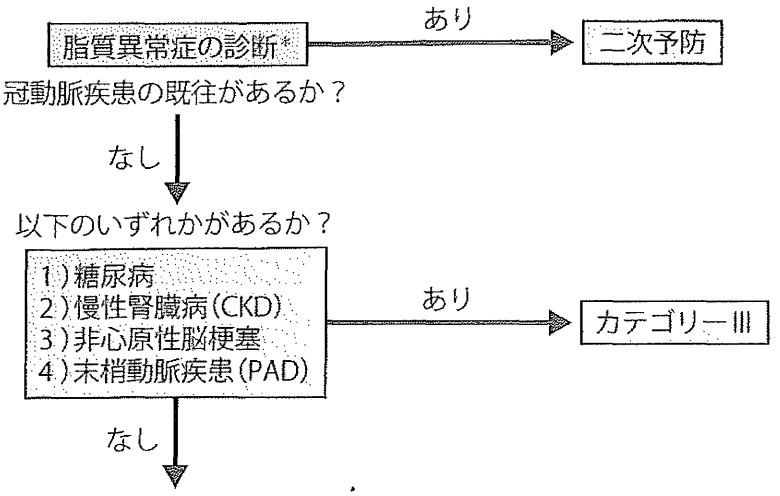

冠動脈疾患の一次予防のための絶対リスクに基づく管理区分

NIPPON DATA80による10年間の冠動脈疾患による死亡確率(絶対リスク)	追加リスクの有無	
	追加リスクなし	以下のうちいずれかあり 1)低HDL-C血症(HDL-C<40mg/dL) 2)早発性冠動脈疾患家族歴 (第1度近親者 かつ 男性55歳未満, 女性65歳未満) 3)耐糖能異常
0.5%未満	カテゴリーI	カテゴリーII
0.5以上2.0%未満	カテゴリーII	カテゴリーIII
2.0%以上	カテゴリーIII	カテゴリーIII

*家族性高コレステロール血症, 75歳以上については本フローチャートを適用しない.

図2-12 LDL-コレステロール管理目標設定のためのフローチャート

(日本動脈硬化学会, 編. 動脈硬化性疾患予防ガイドライン2012年版. 東京: 杏林舎; 2012)[1)]

表2-14 リスク区分別脂質管理目標値

治療方針の原則	管理区分	脂質管理目標値(mg/dL)			
		LDL-C	HDL-C	TG	non HDL-C
一次予防 まず生活習慣の改善を行った後, 薬物療法の適応を考慮する	カテゴリーI	<160	≧40	<150	<190
	カテゴリーII	<140			<170
	カテゴリーIII	<120			<150
二次予防 生活習慣の是正とともに, 薬物療法を考慮する	冠動脈疾患の既往	<100			<130

LDL-Cは20～30%の低下を目標とすることも考慮する.
non HDL-Cの値は, 高TG血症の場合にLDL-Cの管理目標を達成したのちの二次目標である.
TGが400mg/dL以上, 食後採血の場合はnon HDL-Cを用いる.
カテゴリーIで薬物療法の適応を考慮するLDL-Cの基準は180mg/dL以上とする.
(日本動脈硬化学会, 編. 動脈硬化性疾患予防ガイドライン2012年版. 東京: 杏林舎; 2012)[1)]

ステロール血症は，低栄養や全身状態の悪化の指標となる．TCは，栄養サポートチームNutrition Support Team(NST)が入院患者の栄養評価をする際の検査指標としてしばしば用いられる．

異常値を生じるメカニズム

高コレステロール血症は，1)小腸でのコレステロール吸収の亢進，2)肝臓でのコレステロール合成亢進，3)肝臓へのLDLの取り込み低下〔LDL受容体の異常やPCSK9(proprotein convertase subtilisin/kexin type 9)の機能亢進など〕のいずれか，またはこれらの組み合わせで生じる．一方，低コレステロール血症は，1)腸管での吸収不良，2)肝臓での合成低下，3)肝臓へLDLの取り込み亢進(脂質低下剤やPCSK9の機能低下など)で起こる．

異常値を示す疾患・病態

▶異常高値を示す場合

- 原発性高脂血症(家族性高コレステロール血症，家族性複合型高脂血症，家族性Ⅲ型高脂血症など)
- 二次性高脂血症(ネフローゼ症候群，甲状腺機能低下症，Cushing症候群，原発性胆汁性肝硬変，急性間欠性ポルフィリン症など)
- 薬物服用者(ステロイドやシクロスポリンなど)

▶異常低値を示す場合

- 原発性低脂血症(MTP欠損症，家族性低βリポ蛋白血症など)
- 二次性低脂血症(甲状腺機能亢進症，低栄養，Addison病，肝硬変など)

検査のピットフォール

LDLの組成が正常と著しく異なるか，LDLが極端に低値となる場合は，LDL-C直接法でLDL-Cを測定できない〔例：原発性胆汁性肝硬変などの胆汁うっ滞性肝障害，800～1,000 mg/dL以上の著明な高TG血症，Ⅰ型およびⅢ型高脂血症(TGの値にかかわらず)〕．一般的に，LDL-C直接法は食後採血の場合にも測定が可能だが，TGが400～1,000 mg/dLの範囲で正確性に問題がある直接法の試薬があるので注意する[5]．

文献

1) 日本動脈硬化学会，編．動脈硬化性疾患予防ガイドライン2012年版．東京：杏林舎；2012.
2) 平山　哲，他．家族性低βリポタンパク血症．In：先天代謝異常症候群 下―病因・病態研究，診断・治療の進歩―．第2版．東京：日本臨床社；2012. p.112-5.
3) 三井田孝，他．TCとHDL-Cの体位による変化と日内変動についての検討．臨床病理．1996；44：860-4.
4) Friedewald WT, et al. Estimation of the concentration of low-density lipoprotein cholesterol in plasma, without use of the preparative ultracentrifuge. Clin Chem. 1972；18：499-502.
5) Miida T, et al. A multicenter study on the precision and accuracy of homogeneous assays for LDL-cholesterol：Comparison with a beta-quantification method using fresh serum obtained from non-diseased and diseased subjects. Atherosclerosis. 2012；225：208-15.

〈三井田　孝〉

2. 生化学検査　F. 脂質・色素関連物質

43 HDL-コレステロール

基準範囲

- 成人男性・女性：≧40 mg/dL[注1]

[参考上限値]

- HDL-C：100 mg/dL[注2]

生理的変動

HDL-C には日内変動がほとんどないため，食後採血の値を空腹時採血の値に代用できる．

検査の概要・臨床的意義

HDL-C は，従来は 2 価の陽イオンを用いた沈殿法で測定されていたが，現在はほとんどの検査室で HDL-C 直接法により測定されている．LDL-C 直接法と異なり，一般に中程度までの高 TG 血症の影響はほとんどを受けない[2]．

多くの疫学研究の結果から，HDL-C が低いほど，虚血性心疾患や脳梗塞などの動脈硬化性疾患の発症リスクが高くなることが示されている．「動脈硬化性疾患予防ガイドライン 2012 年版」では，HDL-C の管理目標値を 40 mg/dL 以上に定めている[1]．

一方，HDL-C が 100 mg/dL 以上になる高 HDL 血症は，その臨床的意義が定まっていない．少数ではあるが，高 HDL 血症に高 TG 血症を合併すると，虚血性心疾患の発症リスクが高まるという報告がある．コレステリルエステル転送蛋白(CETP)欠損症は，HDL-C が 100 mg/dL 以上の高 HDL 血症の原因として最も多く，完全欠損型では HDL-C が 150～200 mg/dL にも達する．しかし，完全欠損型にも心筋梗塞の報告がある[3]．

異常値を生じるメカニズム

HDL の主要アポ蛋白であるアポリポ蛋白 A-I(アポ A-I)は，肝臓で合成され，脂質に乏しい原始 HDL として分泌される．原始 HDL は，細胞表面に存在する ABCA1(ATP-binding cassette A1)と結合し，細胞膜から遊離型コレステロールを引き抜く．アポ A-I はレシチン・コレステロールアシルトランスフェラーゼ(LCAT)を活性化し，遊離型コレステロールをエステル型コレステロール(CE)に変換する．こうして HDL 粒子の内部に(CE)が蓄積し，HDL は球状の粒子に成熟する．また，球状 HDL は，細胞表面の ABCG1(ATP-binding cassette G1)を介して遊離型コレステロールを引き抜く．この代謝経路のどこかが障害されると，低 HDL 血症をきたす．一方，球状 HDL に蓄積した CE は，VLDL や LDL の TG と，1：1 の比率で CETP により交換される．こうしてできた TG に富む HDL は，肝性リパーゼによって水解を受けて小粒子 HDL に戻る．この経路が障害されると，高 HDL 血症をきたす．

異常値を示す疾患・病態

▶高値を示す場合

- CETP 欠損症，肝性リパーゼ欠損症(きわめて稀)などの原発性脂質異常症

注 1：「動脈硬化性疾患予防ガイドライン 2012 年版」[1]で設定されている病態識別値である．
注 2：一般集団では，男性の 1%未満，女性の約 1～2%がこの上限値を超える．

- 大量飲酒者
- 有酸素運動を行うスポーツ選手
- ステロイドホルモンやインスリン治療を受けている患者の一部

▶低値を示す場合

- 動脈硬化性疾患(虚血性心疾患，虚血性脳梗塞，末梢動脈疾患など)
- 高 TG 血症
- 肥満(特に内臓脂肪型肥満)，メタボリックシンドローム，糖尿病
- 透析患者
- 喫煙者
- 急性および慢性炎症性疾患
- 重症肝機能障害(非代償性肝硬変など)
- LCAT 欠損症，魚眼病，Tangier 病，アポ A-I 欠損症，アポ A-I 異常症など．(HDL-C が 10 mg/dL 未満の著明な低 HDL 血症で疑う)[4]
- 投与薬物の影響(プロブコール，β遮断薬，サイアザイド系降圧利尿薬，向精神薬など)

検査のピットフォール

HDL-C 直接法は，健常人だけでなく，脂質異常症，糖尿病，虚血性心疾患，高血圧など通常の疾患でほぼ正確に HDL-C を測定できる[2]．しかし，胆汁うっ滞性肝疾患や CETP 欠損症などアポ E に富む異常な HDL が増加する病態では，キット間の測定値の差が大きく[5]，HDL-C 直接法では正確な情報が得られない．アポ蛋白など，別の方法で HDL 量を評価する．

検体を長期に保存すると，4℃でも HDL-C の値が変動する．これは，LCAT により遊離型コレステロールがエステル型コレステロールに変換され，CETP によりアポ B 含有リポ蛋白に転送されるためと考えられる．HDL-C 直接法の試薬によって，保存による HDL-C 測定値の変動傾向に差があるので，採血後できるだけ速やかに測定する．

文 献

1) 日本動脈硬化学会，編．動脈硬化性疾患予防ガイドライン 2012 年版．東京：杏林舎；2012.
2) Miida T, et al. Validation of homogeneous assays for HDL-cholesterol using fresh samples from healthy and diseased subjects. Atherosclerosis. 2014; 233: 253-9.
3) 薬師寺恵美，他．冠動脈，頚動脈，末梢動脈すべてに動脈硬化病変を認めたホモ接合体 CETP 欠損症の 1 例．Progress in Medicine, 2012; 32: 2720-7.
4) 三井田孝，他．HDL が異常値を示すときにどう対処するか．Medical Practice. 2005; 22; 1235-40.
5) 杉内博幸，他．HDL-コレステロール，LDL-コレステロール直接測定法の反応特異性に関する最近の研究．生物試料分析．2008: 31; 253-62.

〈三井田　孝〉

ApoE4 Determines the Reduction in LDL-C After GH Replacement Therapy in Children With an Idiopathic GH Deficiency

Hironori Nagasaka, Satoshi Hirayama, Mayuko Takuwa, Mariko Nakacho, Tohru Yorifuji, Hiroki Kondou, and Takashi Miida

Department of Pediatrics (H.N., M.T., M.N.), Takarazuka City Hospital, Hyogo 665-0827, Japan; Department of Clinical Laboratory Medicine (S.H., T.M.), Juntendo University Graduate School of Medicine, Tokyo 113-8421, Japan; Department of Pediatric Endocrinology and Metabolism (T.Y.), Children's Medical Center, Osaka City General Hospital, Osaka 534-0021, Japan; and Department of Pediatrics (H.K.), Nara Hospital, Kinki University Faculty of Medicine, Nara 630-0293, Japan

Context: GH activates the expression of low-density lipoprotein (LDL) receptors, leading to decreased LDL-cholesterol (LDL-C). Apolipoprotein (apo) E4 carriers suppress LDL receptor expression, rendering high LDL-C concentrations.

Objectives: We examined whether GH-deficient children carrying apoE4 exhibited a greater reduction in LDL-C after GH replacement therapy.

Design and Setting: We determined lipoprotein profiles after 0, 4, and 12 months of GH treatment in children with an idiopathic GH deficiency. We compared the effects of GH treatment on LDL-C by apoE phenotype.

Subjects: In total, 66 children with idiopathic GH deficiency and 89 healthy children were classified into subgroups according to apoE phenotype.

Intervention: The intervention included GH replacement therapy for 12 months.

Main Outcome Measures: The relationship between apoE phenotype and reduced LDL-C induced by GH treatment was measured.

Results: Concentrations of LDL-C and apoB were highest in the apoE4/3 group (n = 13), second highest in the apoE3/3 group (n = 46), and lowest in the apoE3/2 group (n = 7), whereas apoE concentrations were highest in the apoE3/2 group and lowest in the apoE4/3 group. The apoE4/3 group had significantly reduced LDL-C and apoB concentrations at months 4 and 12, whereas the apoE3/3 and apoE3/2 groups showed no changes. LDL-C concentrations did not differ among the three groups after 12 months. The trend in apoE concentration did not change among the groups.

Conclusions: Children with a GH deficiency carrying apoE4 had higher baseline LDL-C concentrations and experienced a greater reduction in LDL-C after GH replacement therapy than those without apoE4. **(*J Clin Endocrinol Metab* 100: 3494–3501, 2015)**

GH therapy is widely used to treat patients with primary and secondary GH deficiency (1–5). A large number of children with short stature due to insufficient GH secretion have received GH replacement therapy (2–4). GH promotes the growth of bone growth plates and has several actions unrelated to growth (eg, lipid and carbohydrate metabolism) (1–5). After binding to the GH receptor, GH stimulates downstream intracellular signal-

ISSN Print 0021-972X ISSN Online 1945-7197
Printed in USA

Received January 22, 2015. Accepted June 22, 2015.
First Published Online June 29, 2015

Abbreviations: apoE, apolipoprotein E; CETP, cholesteryl ester transfer protein; CV, coefficient of variation; HbA1c, glycated hemoglobin; HDL-C, high-density lipoprotein cholesterol; LCAT, lecithin-cholesterol acyltransferase; LDL, low-density lipoprotein cholesterol; LDL-C, LDL cholesterol; TC, total cholesterol; TG, triglyceride; VLDL, very low-density lipoprotein.

ing pathways linked to various metabolic functions (6, 7). GH replacement therapy ameliorates hypercholesterolemia in patients with GH deficiency, particularly in adults (1–5, 8). However, the effect of GH on the regulation of low-density lipoprotein cholesterol (LDL-C) levels remains unknown.

Several gene polymorphisms involved in lipoprotein metabolism are associated with changes in the lipoprotein profile before and after GH replacement therapy (8). Apolipoprotein E (apoE), a glycoprotein of 299 amino acids carried on various lipoproteins, is bound to very low-density lipoprotein (VLDL) and is secreted from the liver (9). VLDL is hydrolyzed by lipoprotein lipase, which converts it into VLDL remnants, apoE-rich metabolites of VLDL. ApoE on lipoprotein particles functions as a lipoprotein receptor ligand, promoting their removal from the circulation. Three major isoforms (apoE2, apoE3, and apoE4) occur in the general population and are encoded by the $\epsilon 2$, $\epsilon 3$, and $\epsilon 4$ alleles, respectively. Because human cells have two copies of the apoE gene, one derived from each parent, six common phenotypes (apoE2/2, apoE3/2, apoE3/3, apoE4/2, apoE4/3, and apoE4/4) are observed in the general population. ApoE2, apoE3, and apoE4 contain cysteine/cysteine, cysteine/arginine, and arginine/arginine at residues 112 and 158, respectively. Such substitutions are related to differences in low-density lipoprotein (LDL) receptor affinity and the conversion rate of VLDL to LDL (9).

ApoE phenotypes are closely associated with LDL-C concentrations (10–12). Because apoE4 has a high affinity for hepatic remnant receptors, VLDL remnants deliver their cholesterol to the liver at a higher rate (13, 14). The increased uptake of remnant-derived cholesterol down-regulates the LDL receptor (9), whereas the opposite is true regarding apoE2 carriers, which have little affinity for the hepatic remnant receptor (13, 14). In fact, apoE4 carriers tend to have high concentrations of LDL-C, whereas apoE2 carriers have low concentrations (10–12). However, the effects of apoE4 carriers on LDL-C concentrations are not as clear in children as in adults (12, 15–21). The effects of GH on LDL-C concentrations might depend on the apoE phenotype (1–5, 8, 22). Thus, in the present study, we compared baseline and posttreatment lipoprotein profiles according to apoE phenotype in 66 children with an idiopathic GH deficiency who received 12 months of GH replacement therapy.

Materials and Methods

Subjects

The subjects were 66 children with idiopathic GH deficiency aged 4–9 years who were referred to our hospital for treatment. All of the children met the inclusion criteria of not being obese (<30% overweight) and being euthyroid and prepubertal. Patients who had experienced special episodes, such as asphyxia or respiratory difficulties as newborns and/or infants, were excluded. According to medical records, all of the subjects had normal intellectual development. After visiting neighboring rural hospitals at 3–6 years of age with the chief concern of short stature, they had been referred to our hospital for growth defects. None of the children had an intracranial tumor, based on magnetic resonance imaging. Peak GH concentrations in the serum, determined by chemiluminescence enzyme immunoassay (Access human GH kit; Beckman Coulter Inc), were low (<6 ng/mL) in all of the patients after at least two GH stimulation tests with arginine, clonidine, and insulin. The intra- and interassay coefficients of variation (CVs) for GH were less than 4.0%. Under a diagnosis of GH deficiency manifested as short stature, the children received sc injections of GH 6–7 d/wk at a weekly dose of 0.175 mg/kg. Anthropometric indices and biochemical parameters related to lipid and glucose metabolism were measured after 4 and 12 months of GH treatment.

Our study protocol was approved by a relevant institutional review board. Informed consent was obtained from the children's parents before enrollment.

Determination of apoE phenotype

The apoE phenotypes were determined by isoelectric focusing and immunoblotting (15). Serum samples were dissolved in 0.005 M dithiothreitol plus 0.5% Tween 20 solution and electrofocused at 8°C for 2000 Vh on a 5% polyacrylamide gel containing 5% ampholyte and 3 M urea. The apoE bands were blotted onto nitrocellulose membranes and detected with anti-human apoE polyclonal antibody (AB947; EMD Millipore) as a primary antibody. Immunoelectrophoresis revealed that this antibody is monospecific for apoE and reacts with apoE2, apoE3, and apoE4 by Western blotting (15).

Measurement of lipoproteins and their related enzymes

Blood samples were obtained after an overnight fast using INSEPAC II-D tubes (Sekisui Medical) without anticoagulant. Concentrations of total cholesterol (TC) and triglycerides (TGs) were determined enzymatically (Aqua Auto Kainos T-CHO and Aqua Auto Kainos TG-II; Kainos Laboratories). Levels of high-density lipoprotein cholesterol (HDL-C) and LDL-C were measured using homogeneous assays (Choletest N HDL and Choletest LDL; Sekisui Medical), whose accuracies and precisions were confirmed in previous studies (23, 24). Apolipoprotein concentrations were determined using turbidimetric immunoassays [Apo auto N series (Daiichi); Sekisui Medical]. The activities of lecithin-cholesterol acyltransferase (LCAT) and cholesteryl ester transfer protein (CETP) were determined using commercial kits [Anasorb LCAT and CETP-ELISA (Daiichi); Sekisui Medical]. The intra- and interassay CVs for LCAT are 2.7%–5.2% and 4.5%–6.1% (25), and those for CETP are 2.0%–4.0%, and 5.0%–7.0% (26), respectively.

GH and carbohydrate metabolism parameters

Levels of fasting plasma glucose were measured enzymatically. Levels of glycated hemoglobin (HbA1c), insulin, and IGF-1 (in serum) were determined using HPLC (HLC-723G7; Tosoh), enzyme immunoassays (TOSOH-II; Tosoh), and immunoradiometric assays (Somatomedin C-II kit; Mitsubishi Chemicals), respectively. The intra- and interassay CVs for IGF-1 are 5.0% and 8.0% (27), respectively.

Table 1. Prevalence of apoE Phenotypes and ϵ-Alleles in Children With a GH Deficiency and Nonobese Control Children

	Children With an Idiopathic GH Deficiency (n = 66)				Nonobese Healthy Control Children (n = 89)			
ApoE phenotype	E3/2	E3/3	E4/3	Total	E3/2	E3/3	E4/3	Total
Children, n, %	7 (10.6)	46 (69.7)	13 (19.7)	66 (100.0)	11 (12.4)	57 (64.0)	21 (23.6)	89 (100.0)
ϵ-Allele	ϵ2	ϵ3	ϵ4	Total	ϵ2	ϵ3	ϵ4	Total
Alleles, n, %	7 (5.3)	112 (84.8)	13 (9.8)	132 (100.0)	11 (6.2)	146 (82.0)	21 (11.8)	178 (100.0)

ApoE phenotypes were determined by isoelectric focusing and immunoblotting.

Statistical analyses

Data are presented as means ± SDs. Statistical analyses were performed with Statcel 2 add-in software with Excel 2010 (OMS). Differences between groups were detected using a Fisher's exact test for categorical and proportional variables. Differences in continuous variables among the three apoE phenotypes were detected using one-way ANOVA followed by the Tukey-Kramer post hoc or Kruskal-Wallis test, depending on whether the data had a Gaussian distribution. Data collected before and after treatment were compared using the Wilcoxon signed-rank test in the absence of a Gaussian distribution and repeated-measures ANOVA in the presence of a Gaussian distribution, respectively. A value of $P < .05$ was considered statistically significant.

Results

ApoE phenotype and ϵ allele frequencies

Table 1 shows the prevalence of apoE phenotypes and ϵ-alleles in the subjects. Only three major phenotypes (apoE3/2, apoE3/3, and apoE4/3) were detected, and nearly one-fourth of the children with a GH deficiency had the apoE4/3 phenotype. GH-deficient and control children showed similarly distributed apoE phenotypes and ϵ-allele frequencies.

Anthropometric parameters during GH treatment according to apoE phenotype

The mean age of the children with a GH deficiency was significantly younger than that of the control group (Table 2). However, that of the former at the end of the study reached just about same as that of the latter at baseline [7.6 ± 0.6 y vs 8.1 ± 1.7 y (controls)]. All of the children with a GH deficiency had normal body height and weight at birth, and none had been small-for-gestational-age babies, defined as those with height or weight SD scores less than −2 SD. However, children with a GH deficiency began exhibiting short stature and becoming underweight at 1–6 years of age. There was no association between apoE phenotype and growth retardation.

No differences in mean systolic or diastolic blood pressure were detected between the groups [101 ± 1/57 ± 6

Table 2. Anthropometric Parameters According to apoE Phenotype

	Children With an Idiopathic GH Deficiency				Nonobese Healthy Control Children			
Parameters	E3/2 (n = 7)	E3/3 (n = 46)	E4/3 (n = 13)	Total (n = 66)	E3/2 (n = 11)	E3/3 (n = 57)	E4/3 (n = 21)	Total (n = 89)
Age at baseline, y	6.4 (0.8)[a]	6.6 (0.5)[a]	6.7 (0.6)[a]	6.6 (0.6)[a]	7.8 (1.7)	8.2 (1.8)	8.2 (1.7)	8.1 (1.7)
Age at month 12, y	7.4 (0.8)	7.6 (0.5)	7.7 (0.6)	7.6 (0.6)				
M/F	3/4	24/22	7/6	34/32	4/7	30/27	9/12	43/46
Height, cm								
At birth	48.3 (0.9)	48.5 (0.8)	48.8 (1.0)	48.5 (0.7)	No data	No data	No data	No data
(SD scores)	−0.08 (0.25)	−0.05 (0.22)	0.03 (0.19)	−0.05 (0.23)				
Baseline	102.9 (2.2)[a]	103.0 (2.1)[a]	102.8 (2.0)[a]	102.9 (1.7)[a]	123.9 (10.5)	125.4 (10.3)	126.6 (12.4)	125.5 (10.9)
(SD scores)	−2.78 (0.33)	−2.85 (0.25)	−2.91 (0.25)	−2.86 (0.24)	−0.01 (0.27)	−0.03 (0.22)	0.05 (0.27)	−0.01 (0.22)
Month 4	105.1 (2.3)	105.4 (2.2)	105.2 (2.3)	105.3 (1.9)				
(SD scores)	−2.53 (0.33)	−2.50 (0.24)	−2.54 (0.27)	−2.54 (0.27)				
Month 12	111.4 (2.4)	112.3 (2.1)	111.7 (2.2)	111.9 (1.9)				
(SD scores)	−1.81 (0.29)	−1.92 (0.22)	−2.13 (0.24)	−1.95 (0.26)				
Body weight, kg								
At birth	2.92 (0.15)	2.92 (0.23)	2.98 (0.24)	2.94 (0.23)	No data	No data	No data	No data
(SD scores)	−0.04 (0.24)	−0.03 (0.21)	0.01 (0.33)	−0.03 (0.2)				
Baseline	14.5 (1.1)[a]	14.7 (1.1)[a]	14.3 (0.9)[a]	14.6 (0.8)[a]	24.6 (6.6)	25.5 (5.4)	25.8 (6.3)	25.5 (5.8)
(SD scores)	−2.28 (0.37)	−2.19 (0.31)	−1.97 (0.28)	−2.15 (0.30)	−0.04 (0.26)	−0.05 (0.198)	−0.09 (0.22)	−0.06 (0.22)
Month 4	16.2 (1.2)	16.4 (1.0)	16.0 (1.0)	16.3 (1.0)				
(SD scores)	−2.16 (0.37)	−2.13 (0.29)	−2.18 (0.32)	−2.15 (0.28)				
Month 12	20.5 (1.5)	21.3 (1.2)	20.2 (1.3)	20.9 (0.8)				
(SD scores)	−1.99 (0.35)	−1.85 (0.23)	−1.91 (0.23)	−1.89 (0.24)				

Abbreviations: F, female; M, male. Data are means (standard deviations).

[a] $P < .01$ vs same apoE phenotype group in the control children and overall control children.

mm Hg vs 104 ± 8/54 ± 7 mm Hg (controls)], and no changes in blood pressure were observed before or after GH treatment among apoE phenotypes. Although the GH reference interval is slightly narrower in male than in female children, no difference in the sex ratio was observed among apoE phenotypes or between the treatment and control groups.

Baseline and posttreatment lipoprotein profiles according to apoE phenotype

The apoE4/3 group of children with a GH deficiency had the highest baseline concentrations of TC, followed by the apoE3/3 group and then the apoE3/2 group. In contrast, no differences in TC concentrations by apoE phenotype were found among control children (Table 3). Four months of GH replacement therapy in children with a GH deficiency induced a 7% reduction in TC concentration in the apoE4/3 group and a 3% reduction in the apoE3/3 group, but no change was observed in the apoE3/2 group. TC levels in all of the groups had decreased by month 4 and were comparable with those at month 12. Similarly, posttreatment TC levels in children with a GH deficiency were similar to those in the control group. These changes in TC were mainly due to changes in LDL-C concentrations. The percentage change in TC was positively associated with changes in LDL-C in the apoE4/3 group ($R = 0.54$, $P = .05$ at 4 mo; $R = 0.70$, $P = .007$ at 12 mo). Levels of LDL-C were highest in the apoE4/3 group of children with a GH deficiency, followed by the apoE3/3 group and the apoE3/2 group. In contrast, the apoE phenotype was not associated with LDL-C concentrations in the control group. Only the apoE4/3 and apoE3/3 groups showed significant reductions in LDL-C (8.4% and 5.3%, respectively) after 4 months of GH replacement therapy. However, levels remained stable between months 4 and 12. Concentrations were highest in the apoE4/3 group after month 12. GH replacement therapy tended to increase HDL-C levels to the same degree in all of the apoE phenotypes.

ApoB and apoAI concentrations changed in parallel with changes in LDL-C and HDL-C concentrations. Throughout therapy, the concentrations of apoB were highest in the apoE4/3 group, followed by the apoE3/3 and apoE3/2 groups. In contrast, apoAI concentrations did not differ by apoE phenotype. Levels of TGs and apoE were highest in the apoE3/2 group before GH treatment. Notably, the TG concentrations did not change significantly during therapy, whereas the apoE concentrations increased significantly in the apoE4/3 and apoE3/3 groups at month 4 (Table 3).

GH treatment induced a small but significant reduction in CETP levels (Table 3), but had no effects on LCAT activity [80% ± 4% (baseline) vs 80% ± 5% (month 12)].

Baseline and posttreatment carbohydrate parameters according to apoE phenotype

Although GH replacement therapy induced a marked increase in IGF-1 concentrations (Table 3), it had no effects on carbohydrate parameters. Furthermore, no correlations were found between baseline or posttreatment levels of these parameters and apoE phenotype. IGF-1 concentrations increased to almost twice those at baseline by month 4 in all of the apoE phenotypes and remained high at month 12 [97 ± 13 ng/mL (baseline) vs 172 ± 18 ng/mL, $P < .01$ (month 4) vs 176 ± 19 ng/mL, $P < .01$ (month 12)]. In contrast, therapy did not affect fasting plasma glucose, HbA1c, or serum insulin levels.

Discussion

The results of our study clearly indicate that children with a GH deficiency and apoE4 have higher LDL-C concentrations before GH replacement therapy and experience a greater reduction in LDL-C levels after GH replacement therapy than children with a GH deficiency and one of the other isoforms. The baseline LDL-C concentration of the apoE4/3 group was the greatest of the three major phenotypes and subsequently decreased twice as much as that of the apoE3/3 group, whereas the apoE3/2 group experienced no reduction at all (Table 3). As a result, the mean posttreatment LDL-C concentrations in all of the GH-deficient groups together and the control group were almost identical. Notably, the mean age of children with GH deficiency at the end of the study was similar to that of the control group at baseline.

Earlier studies have shown that diseased children carrying apoE4 have higher concentrations of LDL-C than those carrying apoE3/3 or apoE3/2 (12, 28, 29). In a study of 35 children with type 1 diabetes aged 5–12 years, apoE4 was associated with higher LDL-C levels in those with HbA1c greater than 8.0% (28), whereas those with HbA1c less than 8.0% had rather low levels (78 ± 12 mg/dL) compared with the apoE3/3 group (103 ± 5 mg/dL). In a study on 138 children with type 1 diabetes (mean age 10.2 y; range 2–17 y; HbA1c 8.7%–9.3%), those with apoE4/3 had the highest concentrations of LDL-C, followed by those with apoE3/3 and apoE3/2 (29). We found the same association between LDL-C levels and apoE phenotype because children with a GH deficiency and apoE4/3 had the highest LDL-C levels, followed by those with apoE3/3 and apoE3/2 (Table 3).

These findings imply that apoE4 increases LDL-C levels in the presence of actions and disorders that increase metabolic burden, such as high fat intake, obesity, and glucose metabolic disorders. We speculate that GH decreases

Table 3. Effects of GH Replacement Therapy on Lipoprotein Parameters in Children With a GH Deficiency According to apoE Phenotype

	Children With an Idiopathic GH Deficiency				Nonobese Healthy Control Children			
Parameters	**E3/2 (n = 7)**	**E3/3 (n = 46)**	**E4/3 (n = 13)**	**Total (n = 66)**	**E3/2 (n = 11)**	**E3/3 (n = 57)**	**E4/3 (n = 21)**	**Total (n = 89)**
TC, mg/dL								
Baseline	165 (18)	176 (19)	187 (17)[a,b]	177 (20)[c,d]	167 (11)	173 (21)	167 (17)	171 (19)
Month 4	163 (15)	171 (14)[e]	173 (12)[e]	170 (14)[e]				
Month 12	163 (19)	170 (15)[e]	174 (11)[e]	170 (15)[e]				
LDL-C, mg/dL								
Baseline	84 (15)	95 (19)	107 (19)[b,c]	96 (19)[d]	87 (11)	91 (17)	91 (14)	91 (16)
Month 4	83 (11)	90 (14)[e]	96 (15)[e]	90 (14)[e]				
Month 12	83 (15)	90 (14)[e]	98 (16)[e]	91 (15)[e]				
TG, mg/dL								
Baseline	79 (8)	68 (19)	70 (14)	70 (18)	No data	No data	No data	No data
Month 4	79 (7)	69 (17)	72 (14)	71 (16)				
Month 12	80 (9)	72 (16)	72 (13)	73 (15)				
HDL-C, mg/dL								
Baseline	61 (8)	60 (9)[c]	58 (9)	60 (9)[c]	63 (7)	66 (13)	59 (10)	64 (12)
Month 4	64 (7)	61 (9)	60 (9)	61 (9)				
Month 12	64 (8)	62 (9)	60 (8)	62 (8)				
ApoA-I, mg/dL								
Baseline	141 (8)	136 (12)	137 (11)	137 (11)	141 (9)	144 (18)	136 (15)	142 (17)
Month 4	139 (7)	139 (11)	139 (11)	139 (11)				
Month 12	143 (11)	139 (11)	138 (8)	139 (10)				
ApoB, mg/dL								
Baseline	71 (10)	78 (11)	84 (11)[b]	78 (12)[d]	75 (11)	77 (15)	77 (14)	76 (15)
Month 4	70 (7)	74 (9)[e]	79 (11)[e]	74 (9)[e]				
Month 12	70 (9)	75 (9)[e]	79 (11)[e]	75 (9)[e]				
ApoE, mg/dL								
Baseline	5.3 (0.6)	4.2 (1.0)[b]	3.4 (1.1)[f,g]	4.2 (1.2)[h]	5.5 (0.7)	4.0 (0.9)	3.5 (0.8)	4.1 (1.0)
Month 4	5.5 (0.5)	4.4 (1.1)[be]	3.8 (1.0)[e,f]	4.4 (1.1)[e,h]				
Month 12	5.5 (0.4)	4.4 (1.1)[b]	3.7 (0.8)[f]	4.3 (1.1)[e,h]				
CETP, μg/mL								
Baseline	2.5 (0.3)	2.5 (0.4)	2.6 (0.3)	2.6 (0.4)	No data	No data	No data	No data
Month 12	2.4 (0.3)	2.4 (0.3)[e]	2.4 (0.3)[i]	2.4 (0.3)[e]				

Data are means (SDs).

[a] $P < .01$ vs same apoE phenotype group in control children.

[b] $P < .05$ vs apoE 3/2 in children with a GH deficiency.

[c] $P < .05$ vs same apoE phenotype group in control children.

[d] $P < .05$ by ANOVA among the three groups according to apoE phenotype in children with a GH deficiency.

[e] $P < .01$ vs baseline levels in the same apoE phenotype group in children with a GH deficiency and all children with a GH deficiency.

[f] $P < .01$ vs apoE 3/2 in children with a GH deficiency.

[g] $P < .05$ vs apoE3/3 in children with a GH deficiency.

[h] $P < .01$ by ANOVA among the three groups according to apoE phenotype in children with a GH deficiency.

[i] $P < .05$ vs baseline levels in the same apoE phenotype group in children with a GH deficiency and all children with a GH deficiency.

LDL-C concentrations by up-regulating the activity of LDL receptors, which is crucial to the process of removing circulating LDLs. GH replacement therapy reduces LDL-C concentrations in adults with a GH deficiency (1–5, 8, 22). In one of those studies, levels decreased by 13% and the fractional catabolic rate of LDL increased by 27% in nine healthy young men before and 3 weeks after GH treatment (5). These changes were found in heterozygotes but not homozygotes of familial hypercholesterolemia, supporting the hypothesis that GH up-regulates ex-

pression of the LDL receptor. In contrast, in a study of patients with acromegaly, a rare disease characterized by the presence of excess GH after puberty, apoE4 (apoE4/4 and apoE4/3) carriers had even lower LDL-C concentrations than those of apoE3/3 and apoE2 (apoE3/2 and apoE2/2) carriers (30).

Considering that VLDL-containing apoE4 particles are removed from plasma more rapidly than VLDL containing apoE3 particles, the expression of hepatic LDL receptors in apoE4 carriers is down-regulated due to the accumulation of cholesterol derived from VLDL remnants in the liver (9, 13, 14, 31). Thus, it is reasonable to expect an association between GH and reduced LDL-C levels mediated by LDL receptors in this patient group. In the present study, although reduced LDL-C levels were achieved after 4 months of GH replacement therapy and the level decreased only slightly in the apoE4/3 group, it is notable that the reduction was maintained for 12 months after therapy. The male to female ratio among the groups may have affected our results, but we found no significant difference in the ratio among the apoE phenotypes in children with a GH deficiency.

In previous studies, the effects of apoE4 on LDL-C levels were less evident in healthy children, although the results depended on age, race, and sex (12, 15–21). In a study on 206 Finnish newborns, no differences in LDL-C concentrations were observed among apoE phenotypes (15). In a subsequent examination of 3-year-old children (n = 253), the same study found that LDL-C levels increased with apoE phenotype in a specific order of apoE3/2, apoE3/3, apoE4/3, and apoE4/4, which was independent of sex. A Spanish study of children aged 6–7 years showed the same relationship between apoE genotype and LDL-C concentration (19), but the relationship was more evident in girls than in boys. In a study on 647 African-American girls aged 9–10 years, mean LDL-C concentrations were only 4.3 mg/dL higher in the apoE4/3 group than in the apoE3/3 group (20). In a subsequent examination of 573 Caucasian girls of the same age, the mean concentrations were 2.0 mg/dL lower in the apoE4/3 group than in the apoE3/3 group. However, in both groups, the mean concentrations were 8–10 mg/dL lower in the apoE3/2 group than in the apoE3/3 group.

A study on 91 healthy, nonobese Japanese children (mean age 9.9 ± 0.4 y) did not find a significant association between apoE phenotype and LDL-C concentrations (12), similar to the Finnish study (15) and research on Italian girls (21). In contrast, obese children with the apoE4/3 phenotype have higher concentrations of both TC and LDL-C compared with those with other phenotypes (11% and 12% higher than apoE3/3 and 17% and 26% higher than apoE3/2) (12). The effects of apoE4 on LDL-C levels were clearer in Spanish subjects with high baseline concentrations than in those with low baseline levels (19).

In the present study, apoE phenotype was not associated with LDL-C concentrations in control children. This may be because healthy children have much higher GH concentrations than adults, and GH increases hepatic LDL receptor activity, promoting hepatic LDL uptake (5–7). In addition, young children exhibit rapid growth and development, which requires much higher cholesterol concentrations than the levels found in adults. Cholesterol is an essential constituent of the cell membrane, and the amount must double during cell division, leading to enhanced demand for cholesterol that may offset its association with increased LDL-C levels in healthy children with apoE4.

We also found that apoE concentrations were highest in the apoE3/2 group and lowest in the apoE4/3 group (Table 3). However, the increase was not associated with the reduction in LDL-C at month 4 ($R = 0.34$, $P = .24$). Earlier studies have clearly shown that apoB, not apoE, is a crucial determinant for VLDL synthesis (32); thus, the differences in VLDL metabolism among apoE phenotypes may affect the GH response to the reduction of LDL-C in children with a GH deficiency.

High baseline LDL-C levels and enhanced reduction of LDL-C after GH therapy in apoE4 carriers are likely related to the clearance and conversion rates of VLDL remnants. In general, apoE-containing lipoproteins [chylomicrons, VLDL, intermediate density lipoprotein (IDL)] are taken up by the liver through receptors that recognize apoE (13, 14). The remaining VLDL and IDL remnants are converted to LDL (9). Gregg et al (33) isolated apoE from apoE4 and apoE3 homozygotes (apoE4/4 and apoE3/3), and injected the radiolabeled apoE reassociated with VLDL into the apoE3 homozygotes simultaneously. They found that the residence time for apoE4/4-VLDL was shorter than that for poE3/3-VLDL (0.37 ± 0.01 vs 0.73 ± 0.05 d) (33). Because LDL lacks apoE, these data suggest that apoE4/4-VLDL remnants are cleared more rapidly by the liver than apoE3/3-VLDL. As a result, apoE4/4-VLDL increases the intrahepatic cholesterol pool more than apoE3/3-VLDL. If this is true, LDL receptor expression is down-regulated in the liver of apoE4 carriers.

In another kinetic study, radiolabeled $VLDL_1$ and $VLDL_2$ were injected into apoE2, apoE3, and apoE4 homozygous subjects, and blood samples were collected repeatedly until day 14 (34). ApoB and apoE in $VLDL_1$, $VLDL_2$, IDL, and LDL were separated by density gradient ultracentrifugation followed by a tetramethylurea precipitation method. Kinetic parameters were calculated using a multicompartment model. The percentage of VLDL con-

verted to LDL was higher in apoE4 homozygotes than that in apoE2 or apoE3 homozygotes (70% ± 14% vs 23% ± 8% and 50% ± 13%, respectively). These kinetic features explain the high baseline LDL-C concentrations in apoE4 carriers. In contrast, apoE2 has little affinity for remnant receptors despite high concentrations, and VLDL remnants that are rich in cholesterol, such as IDLs, are not efficiently removed by the hepatic receptors in apoE2 carriers (31, 33, 34). Thus, intrahepatic cholesterol content remains low, leading to the up-regulated expression of LDL receptors in apoE2 carriers (9, 13, 14). These differences in the activity and/or expression of LDL receptors may explain why GH replacement therapy causes a reduction in LDL-C levels that is dependent on apoE phenotype in children with a GH deficiency.

In summary, our findings indicate that the apoE phenotype is more strongly associated with lipoprotein profiles in children with a GH deficiency than in those without one. Furthermore, children with a deficiency and particular phenotypes have higher LDL concentrations but experience greater reductions in LDL-C levels after GH replacement therapy. In particular, children with a deficiency and the apoE4 phenotype have higher baseline LDL-C concentrations and experience a greater reduction after therapy than those without the apoE4 phenotype. These results suggest that children with the apoE4 phenotype are at higher risk for developing atherosclerosis, which is often masked by the high demand for cholesterol during the growing years.

Acknowledgments

Address all correspondence and requests for reprints to: Satoshi Hirayama, MD, PhD, Department of Clinical Laboratory Medicine, Juntendo University Graduate School of Medicine, Hongo 2-1-1, Bunkyo-ku, Tokyo 113-8421, Japan. E-mail: sthiraya@juntendo.ac.jp.

Disclosure Summary: The authors have nothing to disclose.

References

1. **Muller N, Jorgensen JO.** Effects of growth hormone on glucose, lipid, and protein metabolism in human subjects. *Endocr Rev.* 2009; 30:152–157.
2. **Kuromaru R, Kohno H, Ueyama N, Hassan HM, Honda S, Hara T.** Long-term prospective study of body composition and lipid profiles during and after growth hormone treatment in GH deficiency: gender-specific metabolic effects. *J Clin Endocrinol Metab.* 1998;83: 3890–3896.
3. **Ciresi A, Amato MC, Criscimanna A, et al.** Metabolic profiles and adipokine profile during GH replacement therapy in children with GH deficiency. *Eur J Endocrinol.* 2007;156:353–360.
4. **Sas T, Mulder P, Hokken-Koelega A.** Body composition, blood pressure, and lipid metabolism before and during long-term growth hormone treatment in children with short stature born for gestational age either with or without GH deficiency. *J Clin Endocrinol Metab.* 2000;85:3786–3792.
5. **Lind S, Rudling M, Ericsson S, et al.** Growth hormone induces low-density lipoprotein clearance but not bile acid synthesis in humans. *Arterioscler Thromb Vasc Biol.* 2004;24:349–356.
6. **Frank SJ.** Growth hormone signalling and its regulation: preventing too much of a good thing. *Growth Horm IGF Res.* 2001;11:201–212.
7. **Vijayakumar A, Novosyadlyy R, Wu Y, Yakar S, LeRoith D.** Biological effects of growth hormone on carbohydrate and lipid metabolism. *Growth Horm IGF Res.* 2010;20:1–7.
8. **Barbosa EJ, Glad CA, Nilsson AG, et al.** Genotypes associated with lipid metabolism contribute to differences in serum lipid profile of GH-deficient adults before and after GH replacement therapy. *Eur J Endocrinol.* 2012;167:353–362.
9. **Davignon J, Gregg RE, Sing CF.** Apolipoprotein E polymorphism and atherosclerosis. *Arteriosclerosis.* 1998;8:1–21.
10. **Miida T.** Apolipoprotein E phenotypes in patients with coronary artery disease. *Tohoku J Exp Med.* 1990;160:177–187.
11. **Zamma MM, Ikemoto S, Yoshiike N, Date C, Yokoyama T, Tanaka H.** Association of apolipoprotein genetic polymorphism with plasma cholesterol in a Japanese population: the Shibata Study. *Arterioscler Thromb Vasc Biol.* 1997;17:3495–3504.
12. **Wardaningsih E, Miida T, Seino U, et al.** Low adiponectin state is associated with metabolic abnormalities in obese children, particularly apolipoprotein E phenotype. *Ann Clin Biochem.* 2008;45: 496–453.
13. **Eichner JE, Dunn ST, Perveen G, Thompson DM, Stewart KE, Stroehla BC.** Apolipoprotein E polymorphism and cardiovascular disease: a HuGE review. *Am J Epidemiol.* 2002;155:487–495.
14. **Weintraub MS, Eisenberg S, Breslow JL.** Dietary fat clearance in normal subjects is regulated by genetic variation in apolipoprotein E. *J Clin Invest.* 1987;80:1571–1577.
15. **Srinivasan SR1, Ehnholm C, Wattigney W, Berenson.** Apolipoprotein E polymorphism and its association with serum lipoprotein concentrations in black versus white children: the Bogalusa Heart Study. *Metabolism.* 1993;42:381–386.
16. **Hu P, Qin YH, Lei FY, Pei J, Hu B, Lu L.** Variable frequencies of apolipoprotein E genotypes and its effect on serum lipids in the Guangxi Zhuang and Han children. *Int J Mol Sci.* 2011;12:5604–5615.
17. **Smart MC, Dedoussis G, Louizou E, et al.** APOE, CETP and LPL genes show strong association with lipid levels in Greek children. *Nutr Metab Cardiovasc Dis.* 2010;20:26–33.
18. **Nghiem NT, Ta TT, Ohmori R, et al.** Apolipoprotein E polymorphism in Vietnamese children and its relationship to plasma lipid and lipoprotein levels. *Metabolism.* 2004;53:1517–1521.
19. **Garcés C, Benavente M, Lasunción MA, Ortega H, Nájera G, de Oya M.** Gender-specific effects of apolipoprotein E genotype on plasma lipid levels in a population-based sample of 6- to 7-year-old children in Spain. *Acta Paediatr.* 2002;91:1039–1043.
20. **Sanghera DK, Ferrell RE, Aston CE, McAllister AE, Kamboh MI, Kimm SY.** Quantitative effects of the apolipoprotein E polymorphism in a biracial sample of 9- to 10-year-old girls. *Atherosclerosis.* 1996;126:35–42.
21. **Xu CF, Talmud PJ, Angelico F, Del Ben M, Savill J, Humphries SE.** Apolipoprotein E polymorphism and plasma lipid, lipoprotein, and apolipoprotein levels in Italian children. *Genet Epidemiol.* 1991;8: 389–398.
22. **Newman CB, Carmichael JD, Kleinberg DL.** Effects of low dose versus high dose human growth hormone on body composition and lipids in adults with GH deficiency: a meta-analysis of placebo-controlled randomized trials. *Pituitary.* 2015;18:297–305.
23. **Miida T, Nishimura K, Okamura T, et al.** A multicenter study on the precision and accuracy of homogeneous assays for LDL-cholesterol: comparison with a β-quantification method using fresh serum obtained from non-diseased and diseased subjects. *Atherosclerosis.* 2012;225:208–215.

24. **Miida T, Nishimura K, Okamura T, et al.** Validation of homogeneous assays for HDL-cholesterol using fresh samples from healthy and diseased subjects. *Atherosclerosis*. 2014;233:253–259.
25. **Kobori K, Saito K, Ito S, Kotani K, Manabe M, Kanno T.** A new enzyme-linked immunosorbent assay with two monoclonal antibodies to specific epitopes measures human lecithin-cholesterol acyltransferase. *J Lipid Res*. 2002;43:3253–3334.
26. **Miida T, Miyazaki O, Hanyu O, et al.** LCAT-dependent conversion of prebeta1-HDL into α-migrating HDL is severely delayed in hemodialysis patients. *J Am Soc Nephrol*. 2003;14:732–738.
27. **Isojima T, Shimatsu A, Yokoya S, et al.** Standardized centile curves and reference intervals of serum insulin-like growth factor-I (IGF-I) levels in a normal Japanese population using the LMS method. *Endocr J*. 2012;59:771–780.
28. **Tso TK, Snook JT, Lozano RA, Zipf WB.** Risk factors for coronary heart disease in type 1 diabetic children: the influence of apoE phenotype and glycemic regulation. *Diabetes Res Clin Pract*. 2001;54:165–171.
29. **Salo MK, Rantanen R, Huupponen T, Lehtimäki T, Jokela H.** Apolipoprotein E phenotypes and plasma lipids in diabetic children and adolescents. *Eur J Pediatr*. 1993;152:564–568.
30. **Boero L, Manavela M, Meroño T, Maidana P, Gómez Rosso L, Brites F.** GH levels and insulin sensitivity are differently associated with biomarkers of cardiovascular disease in active acromegaly. *Clin Endocrinol (Oxf)*. 2012;77:579–585.
31. **Siest G, Pillot T, Régis-Bailly A, et al.** Apolipoprotein E: an important gene and protein to follow in laboratory medicine. *Clin Chem*. 1995;41:1068–1086.
32. **Fisher EA.** The degradation of apolipoprotein B100: multiple opportunities to regulate VLDL triglyceride production by different proteolytic pathways. *Biochim Biophys Acta*. 2012;1821:778–781.
33. **Gregg RE, Zech LA, Schaefer EJ, Stark D, Wilson D, Brewer HB Jr.** Abnormal in vivo metabolism of apolipoprotein E4 in humans. *J Clin Invest*. 1986;78:815–821.
34. **Demant T, Bedford D, Packard CJ, Shepherd J.** Influence of apolipoprotein E polymorphism on apolipoprotein B-100 metabolism in normolipemic subjects. *J Clin Invest*. 1991;88:1490–1501.

Biochemical and Biophysical Research Communications 463 (2015) 650–655

Contents lists available at ScienceDirect

Biochemical and Biophysical Research Communications

journal homepage: www.elsevier.com/locate/ybbrc

Isopentenyl pyrophosphate secreted from Zoledronate-stimulated myeloma cells, activates the chemotaxis of γδT cells

Eishi Ashihara [a, b, *, 1], Tatsuya Munaka [c, 1], Shinya Kimura [d], Saori Nakagawa [e], Yoko Nakagawa [b], Masaki Kanai [c], Hideyo Hirai [b], Hirohisa Abe [c], Takashi Miida [f], Susumu Yamato [e], Shuichi Shoji [g], Taira Maekawa [b]

[a] Department of Clinical and Translational Physiology, Kyoto Pharmaceutical University, Kyoto, Japan
[b] Department of Transfusion Medicine and Cell Therapy, Kyoto University Hospital, Kyoto, Japan
[c] Technology Research Laboratory, Shimadzu Corporation, Kyoto, Japan
[d] Division of Hematology, Respiratory Medicine and Oncology, Department of Internal Medicine, Faculty of Medicine, Saga University, Saga, Japan
[e] Department of Bio-analytical Chemistry, Faculty of Pharmaceutical Sciences, Niigata University of Pharmacy and Applied Life Sciences, Niigata, Japan
[f] Department of Clinical Laboratory Medicine, Juntendo University School of Medicine, Tokyo, Japan
[g] Department of Electronic and Photonic Systems, Waseda University, Tokyo, Japan

ARTICLE INFO

Article history:
Received 11 May 2015
Accepted 30 May 2015
Available online 3 June 2015

Keywords:
γδT cells
Chemotaxis
Tumor immunity
Multiple myeloma
Isopentenyl pyrophosphate

ABSTRACT

γδT cell receptor (TCR)-positive T cells, which control the innate immune system, display anti-tumor immunity as well as other non-immune-mediated anti-cancer effects. γδT cells expanded *ex vivo* by nitrogen-containing bisphosphonate (N-BP) treatment can kill tumor cells. N-BP inhibits farnesyl pyrophosphate synthase in the mevalonate pathway, resulting in the accumulation of isopentenyl pyrophosphate (IPP), which is a stimulatory antigen for γδT cells. We have previously observed that as they get closer, migrating γδT cells increase in speed toward target multiple myeloma (MM) cells. In the present study, we investigated the γδT cell chemotactic factors involving using a micro total analysis system-based microfluidic cellular analysis device. The addition of supernatant from RPMI8226 MM cells treated with the N-BP zoledronic acid (ZOL) or the addition of IPP to the device induced chemotaxis of γδT cells and increased the speed of migration compared to controls. Analysis of the ZOL-treated RPMI8226 cell supernatant revealed that it contained IPP secreted in a ZOL-dose-dependent manner. These observations indicate that IPP activates the chemotaxis of γδT cells toward target MM cells treated with ZOL.

1. Introduction

γδT cell receptor (TCR)-positive T cells, which control the innate immune system, display anti-tumor immunity as well as other non-immune-mediated anti-cancer effects. We have previously demonstrated that nitrogen-containing bisphosphonate (N-BP) treatment expands γδT cells *ex vivo* and that these expanded cells can kill tumor cells in a major histocompatibility complex (MHC)-unrestricted manner [1–3]. N-BP inhibits farnesyl pyrophosphate synthase in the mevalonate pathway, resulting in the accumulation of isopentenyl pyrophosphate (IPP) [4], which is a stimulatory antigen for γδT cells. γδT cells stimulated by the N-BP zoledronic acid (ZOL) recognize tumor cells via several molecules including IPP, MHC class I-related chain gene A (MICA), ICAM-1, CD166, and CD266 [2,5–8].

Following the Encyclopedia of DNA Elements Projects, the analyses of proteomes as well as cellomes have attracted considerable attention across the life science. Research in these fields has recently focused on the elucidating vital mechanisms for the

Abbreviations: TCR, T cell receptor; N-BP, nitrogen-containing bisphosphonate; MM, multiple myeloma; IPP, isopentenyl pyrophosphate; ZOL, zoledronic acid; MIC-A, MHC class I-related chain gene A; μTAS, micro total analysis system; r, recombinant; h, human; IL, interleukin; HPLC, high-performance liquid chromatography; PB, peripheral blood; PBMC, peripheral blood mononuclear cell; CM, conditioned medium; ECI, Effective Chemotaxis Index; HPLC-MS/MS, high-performance liquid chromatography-tandem mass spectrometry; MRM, multiple reaction monitoring; DMAPP, dimethylallyl pyrophosphate; E:T ratio, effector cell to tumor cell ratio.

* Corresponding author. 5 Nakauchi, Yamashina-ku, Kyoto, 607-8414, Japan.
E-mail address: ash@mb.kyoto-phu.ac.jp (E. Ashihara).

[1] These authors contributed equally.

http://dx.doi.org/10.1016/j.bbrc.2015.05.118
0006-291X/

development of novel therapeutic strategies against various diseases. Essential in parallel is the development of new devices for clarifying the mechanisms of cellular functions, including chemotaxis and secretion of hormones. A transwell chamber system has traditionally been used to analyze cell migration toward stimulators. However, this device is often inadequate in providing a reproducible, controllable, and stable linear gradient. Furthermore, a transwell chamber system is not compatible with live cell imaging [9,10]. To overcome these problems, the lab-on-chip or micro total analysis system (μTAS) has been recently applied. A μTAS controls the microenvironment of cells, enabling their biological behaviors, including chemotaxis, differentiation, and cell–cell interactions, to be analyzed [10–13]. The microvalve is a particularly useful tool for investigating the fast-response of cells [10]. We have developed a micro total analysis system (μTAS)-based microfluidic cellular analysis device, which possesses a minute-volume (240 nL) chamber integrated with a microsample injector controlled by a microvalve that permits the injection of a small amount (several nL) of a solute [14,15]. We have previously demonstrated real-time monitoring of antibody secretion from B cells using this microchip [14]. Moreover, because of the minute size of this chamber, we can analyze the behavior of individual cells in response to stimulators, including drugs and chemokines. Importantly, fluid convection or stirring has no influence on a concentration gradient and the solute can consequently spread in a diffusion-dependent manner (Supplementary Fig. S1). In the present study, we investigated γδT cell chemotaxis using a μTAS-based microchamber device. Our results show that ZOL-treated MM cells secrete the metabolite of mevalonate pathway IPP and that IPP activates the γδT cell migration.

2. Materials and methods

2.1. Reagents

The human RPMI8226 MM cell line was purchased from the Deutsche Sammlung von Mikroorganismen und Zellkulturen GmbH (Braunschweig, Germany) and was cultured in RPMI1640 (Gibco, Tokyo, Japan) containing 10% heat-inactivated FCS (Gibco), L-glutamine (Gibco), and 1% penicillin-streptomycin (Gibco). The synthetic pyrophosphomonoester compound 2-methyl-3-butenyl-1-pyrophosphate was kindly provided by Dr. Yoshimasa Tanaka (Kyoto University, Kyoto, Japan). Recombinant human interleukin-2 (rhIL-2) was provided by Shionogi Inc. (Tokyo, Japan). IPP, ammonium bicarbonate (NH_4HCO_3), and 28% ammonia solution were purchased from Sigma–Aldrich (St. Louis, MO, USA). High-performance liquid chromatography (HPLC) grade 2-propanol and acetonitrile were obtained from Wako Pure Chemical Industries Ltd. (Osaka, Japan). All other chemicals used were of analytical-reagent grade.

2.2. Human γδT cell preparations and culture

Peripheral blood (PB) and human AB serum were collected from healthy volunteers. Approval was obtained from the institutional review board at Kyoto University Hospital and informed consent was provided by all volunteers, according to the Declaration of Helsinki. PB mononuclear cells (PBMCs) were isolated using Ficoll–Paque Plus (GE Healthcare, Tokyo, Japan). The PBMCs were then cultured and γδT cells were expanded using 2-methyl-3-butenyl-1-pyrophosphate and rhIL-2, as described previously [2]. This method ensured expanded PBMC preparations that consisted predominantly of γδT cells (>95%). These cells served as a polyclonal γδT-cell source [2,8].

2.3. Preparation of N-BP stimulated RPMI8226 cell-conditioned medium

To investigate whether the supernatant of RPMI8226 MM cells treated with ZOL induced chemotaxis of γδT cells using a μTAS-based microchamber [14,15], RPMI8226 MM cells were cultured with ZOL (1 μM) overnight. The conditioned medium (CM) was then collected and passed through a 0.22 μm filter (Millipore, Tokyo, Japan). Human γδT cells were obtained by culturing PBMNCs, as previously reported [2]. These cells were cultured in the microchip and 24 nL of the CM supernatant was injected via a microinjector. After injection of the CM, γδT cell migration was observed under a microscope and continuous time-lapse recording was performed in every 30 s for 30 min.

2.4. Quantitative analysis of γδT cell migration in a modified Boyden chamber assay

Prior to applying the μTAS-based microchamber system, the migration of γδT cells was first confirmed in a modified Boyden chamber migration assay using 3.0 μm porous membrane trasnwell inserts (Corning, Tokyo, Japan). γδT cells (5×10^4/mL) were put into upper transwell chambers and IPP was added to the lower chambers at a final concentration of 1 or 5 ng/mL. After 4 h incubation, γδT cells migrated into the lower chambers were counted by the modified MTT assay-based Cell-Counting Kit-8 (Dojindo Laboratory, Kumamoto, Japan) in accordance with manufacturer's instrucions.

2.5. Quantitative analysis of γδT cell migration using a microchamber assay

The migration of γδT cells in the microchamber was examined under a microscope with continuous time-lapse recording as described above. The tracks of cell migration were traced using Image J, an image-processing program in the public domain. To estimate the migration of γδT cells quantitatively, the following indices of chemotaxis were used (Supplementary Fig. S2): (1) Speed: $d/\Delta t$, (2) Effective Chemotaxis Index (ECI): $d \times \cos\theta/\Delta t = \Delta x/\Delta t$. The chemotactic indices of γδT cells were evaluated according to these formulae.

2.6. Measurement of IPP in culture supernatants

The concentrations of IPP in culture supernatants were determined using a sensitive HPLC-tandem mass spectrometry (HPLC-MS/MS) methods [16], as described previously, with slight modification. In brief, culture supernatants were added to 1 mL of 2-propanol:0.1 M NH_4HCO_3 (1:1 v/v) and 1.5 mL of acetonitrile for deproteinization, and then vortexed. The deproteinized samples were kept for 10 min on ice, and then centrifuged for 20 min at 3000 rpm under 4 °C. After centrifugation, supernatants were transferred to glass tubes and then dried under a stream of nitrogen at room temperature. The residues were then dissolved in 40 μL of 0.01 M NH_4OH, and 20 μL aliquot of the solution was injected into the HPLC-MS/MS system. Quantification of IPP was performed by standard addition method. The HPLC system consisted of a gradient pump, a vacuum degasser, a column temperature controller, and an autosampler (Shimadzu, Kyoto, Japan). Column temperature was thermostat-controlled at 30 °C. The samples were injected onto a 2.0 × 50 mm Luna C18(2) column, 3 μm in particle diameter (Phenomenex, Torrance, CA). The IPP were chromatgraphed by a linear gradient between solution A (20 mM NH_4HCO_3 and 0.1% triethylamine) and solution B (acetonitrile and 0.1% triethylamine). The gradient was as follows: 0–5 min, 100% A to 20% A; 5–7 min,

20% A; 7–7.01 min, 20% A to 100% A; 7.01–10 min, 100% A; equilibration with 100% A. The flow rate was set at 0.4 mL/min. Mass spectrometry (MS) detection was performed with an API 3200 MS/MS system (Applied Biosystems, Foster City, CA) in the negative electrospray ionization mode. The ion spray voltage was set at 4500 V, the capillary temperature was 700 °C and the collision energy was −42 eV. IPP was detected with the mass spectrometer in the multiple reaction monitoring (MRM) mode set at m/z 244.80 → m/z 79.00. The HPLC-MS/MS method could not separate and identify the isoforms of IPP and dimethylallyl pyrophosphate (DMAPP) in a similar manner as reported previously [16]. Therefore, the concentration was expressed as the total amount of IPP in the total amount of IPP and DMAPP (IPP/DMAPP).

2.7. Statistics

The differences in the speed of γδT cell migration were analyzed using the *t* test. The dose-dependent effect of IPP on γδT cell migration in conventional transwell chambers was analyzed using Williams' method. A *P*-value of 0.05 was considered statistically significant.

3. Results

3.1. Migration of γδT cells was activated by RPMI8226 CM

To investigate whether RPMI8226 MM cells treated with ZOL secreted chemotactic factors for γδT cells, the CM from RPMI8226 cells treated by ZOL was applied into a microchamber containing γδT cells (5×10^5/mL) via a microinjector. After the injection of the CM, the γδT cell migration was investigated under a microscope and the continuous time-lapse recording was carried out. While γδT cells treated by the 10% FCS-containing culture medium (control) moved randomly (Supplementary Movie S1), the cells treated by the RPMI8226 CM migrated toward the injector (Fig. 1a and Supplementary Movie S2). Moreover, the number of cells with an ECI of >1 μm/min was increased by the injection of CM, compared to the control (Fig. 1b). The speed and ECI of RPMI8226 CM-treated γδT cells (n = 84) were 2.69 ± 0.81 μm/min and 0.89 ± 0.66 μm/min, respectively *vs.* 2.0 ± 0.69 μm/min and 0.22 ± 0.53 μm/min, respectively in the control of γδT cells (n = 39). The speed and ECI of γδT cells after the injection of CM were significantly higher than after the injection of the culture medium ($P < 0.0001$, Fig. 1c). In addition, after treatment with RPMI8226 CM, the γδT cells moved closer to the injector than they did when treated with the control medium (Supplementary Fig. S3). These observations suggest that CM from ZOL-treated RPMI8226 cells contains certain chemotactic factors for γδT cells.

Supplementary video related to this article can be found at http://dx.doi.org/10.1016/j.bbrc.2015.05.118.

3.2. IPP significantly increased the speed of γδT cell migration

We next investigated whether IPP, a metabolite of the mevalonate pathway and known γδT cell stimulatory antigen, activates the γδT cell migration. First we examined the effect of IPP on γδT cell migration using a conventional transwell migration assay in a modified Boyden chamber. By counting the number of γδT cells attracted across the transwell membrane to the lower chamber containing IPP (0, 1 or 5 ng/mL), we determined that IPP induced γδT cell migration in a dose-dependent manner ($P < 0.05$, Supplementary Fig. S4). Next, we investigated the alteration in speed of the γδT cells in response to IPP using the μTAS-based microchamber. We recorded the movement of γδT cell migration and traced their tracks by IPP and the solvent control, and then estimated the chemotactic indices of γδT cells. When the solvent control was injected, γδT cells moved at random. In contrast, the γδT cells moved toward the microinjector when IPP was introduced (Fig. 2a and Supplementary Movies S3 and Supplementary Movies S4). Like the treatment of RPMI8226-CM supernatant, the numbers of cells whose ECIs were more than 1 μm/min were increased by the injection of IPP compared with that by the injection of the solvent control (Fig. 2b). The speed and ECI of IPP-treated γδT cells (n = 51) were 2.89 ± 0.80 and 1.29 ± 0.80 μm/min, respectively. On the contrary, the speed and ECI of solvent-treated γδT cells (n = 53) were 1.92 ± 0.89 and 0.19 ± 0.43 μm/min, respectively. IPP significantly enhanced the γδT cell migration ($P < 1 \times 10^{-5}$; Fig. 2c). After the injection of IPP, the γδT cells moved further toward injector than the cells treated with solvent control (Supplementary Fig. S5). These findings indicate that IPP significantly enhances the chemotactic migration of γδT cells.

Supplementary video related to this article can be found at http://dx.doi.org/10.1016/j.bbrc.2015.05.118.

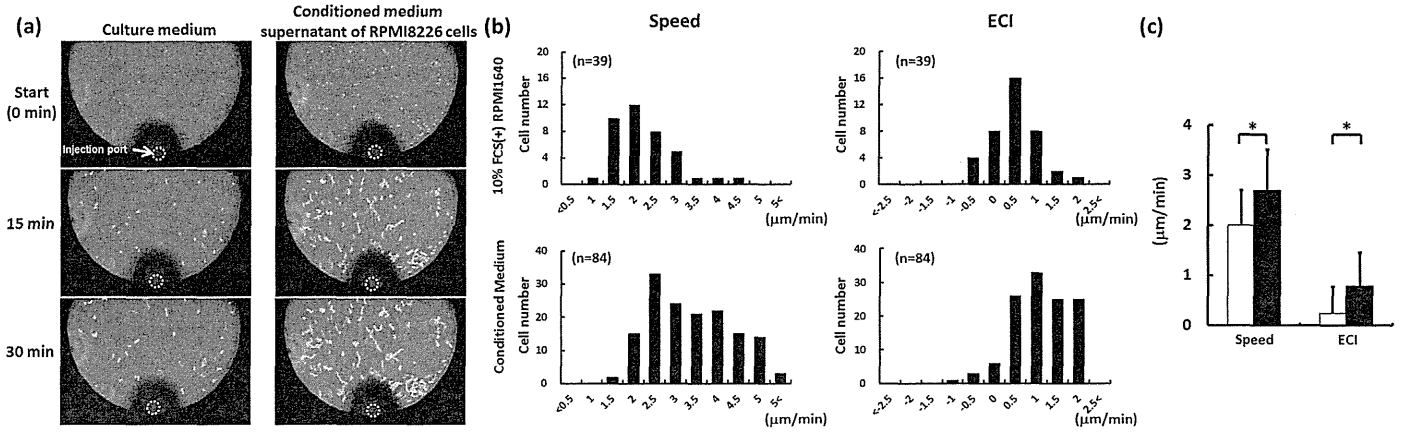

Fig. 1. Quantitative analysis of γδT cell migration induced by RPMI8226-conditioned medium (CM). (a) Tracking γδT cell migration after injection of the 10% FCS-containing culture medium or RPMI8226-CM via the microinjector. Images were captured every 30 s for the indicated times and overlaid. White tracks indicate each γδT cell movement in the time during the indicated time. (b) Histograms of speed and effective chemotaxis index (ECI) of migrating γδT cells. The negative values for speed and ECI indicate γδT cell migration from the initial point in the opposite direction of the microinjector. (c) The mean values of speed and ECI of the γδT cells treated with the medium (white bars) and with RPMI8226-CM (black bars) form the data in b. The data represent means + standard deviations and are representative data of four independent experiments. *P < 0.0001.

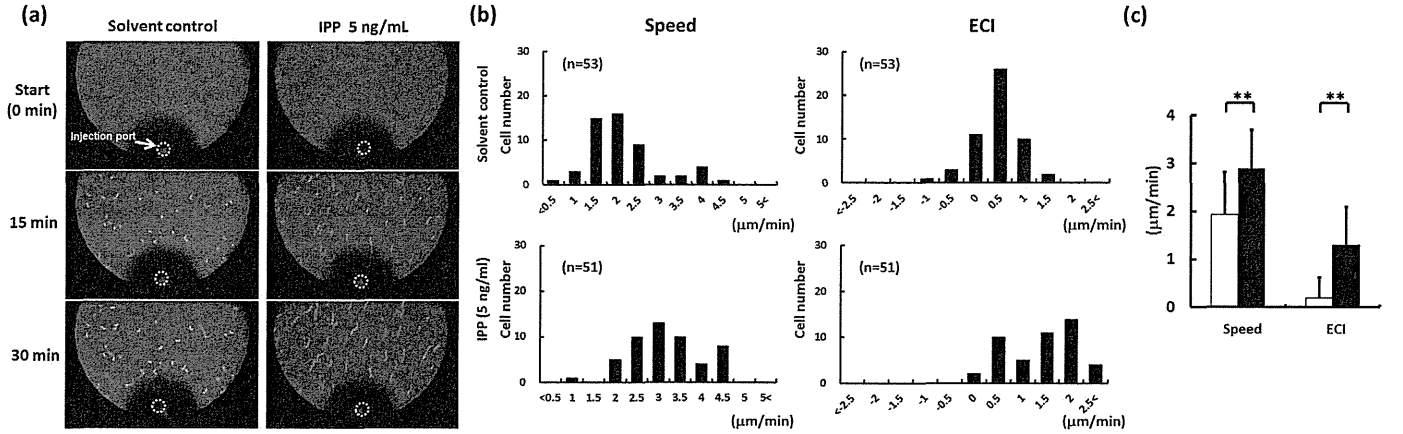

Fig. 2. Quantitative analysis of γδT cell migration induced by Isopentenyl pyrophosphate (IPP). (a) Tracking γδT cell migration after treatment with 5 ng/mL IPP-containing control solvent or control solvents. White tracks indicate each γδT cell movement. (b) Histograms of speed and effective chemotaxis index (ECI) of migrating γδT cells. The negative values for speed and ECI indicate γδT cell migration from the initial points in the opposite direction of the microinjector. (c) The mean values of speed and ECI of migrating γδT-cells induced by IPP (black bars) or solvent control (white bars) form the data in b. The data represent means + standard deviations and are representative data of two independent experiments. $^{**}P < 1 \times 10^{-5}$.

3.3. ZOL-treated RPMI8226 MM cells secreted IPP into the culture medium

Treatment of tumor cells with N-BPs inhibits farnesyl pyrophosphate synthase in the mevalonate pathway, resulting in the accumulation of the γδT-cell stimulatory antigen IPP [4,17]. To determine whether the RPMI8226 MM cells secrete IPP into the supernatant by the ZOL treatment, we measured the IPP concentrations in the supernatants using HPLC-MS/MS as previously described [16]. Although IPP was not detected in the fresh medium containing 10% FCS, the concentrations of IPP in the culture supernatant without ZOL treatment were 1.06 ± 0.02 ng/mL. When the cells were cultured in the presence of ZOL at 1 μM and 5 μM, the concentrations of IPP in the supernatant were 3.24 ± 0.27 ng/mL and 6.15 ± 0.84 ng/mL, respectively (Fig. 3). The IPP concentrations were increased by ZOL treatment in a dose-dependent manner. We also detected IPP in the supernatant of SBC-5 small lung cancer cells. The concentrations of IPP in the supernatant in the presence of ZOL at 0, 1, and 5 μM were 0.60 ± 0.45, 0.79 ± 0.43, and 1.05 ± 0.39 ng/mL, respectively. Taken together, RPMI8226 MM cells secrete IPP into the extracellular fluid by ZOL treatment, and γδT cells migrate toward RPMI8226 cells by the secreted IPP.

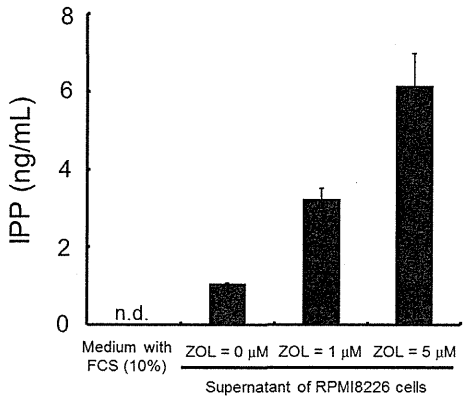

Fig. 3. Concentration of isopentenyl pyrophosphate (IPP) in the supernatant of RPMI8226 myeloma cells. Zoledronic acid was added to 1×10^6 cells at the indicated concentration and the cells were cultured for 18 h. The concentration of IPP in the supernatant was then determined by high-performance liquid chromatography-tandem mass spectrometry. The data represent means + standard deviation of two independent experiments. n.d.; not detected.

4. Discussion

By N-BP treatment, IPP was accumulated on the surface of the tumor cells and IPP activates γδT cells via γδTCRs [1,2,3,4,8,18,19]. In a previous study, we have observed that migrating γδT cells increase their speed toward MM as well as solid cancer target cells as they move closer to them [1,2], and from this we hypothesized that cancer cells secreted the chemotactic factors for γδT cells into the supernatant. We focused on the ZOL-stimulated metabolites in the γδT cells, and we detected IPP in the culture medium of RPMI8226 MM cells by ZOL treatment in a dose-dependent manner (Fig. 3). The previous study demonstrated that high doses of ZOL (more than 10 μM) inhibited the prenylation of Rap1Ain tumor cells [20]. Although the unprenylated Rap1A could be detected scarcely by the ZOL treatment at the concentration of 1 μM, the treatment of ZOL at 1 and 5 μM inhibited the prenylation (Supplementary Fig. S6). Therefore, farnesyl pyrophosphate synthase was inhibited by the treatment of ZOL at low doses of 1 and 5 μM, resulting in the IPP secretion from RPMI8226 MM cells as shown in Fig. 3.

In the present study, using a μTAS-based microchamber, we have shown that CM from N-BP-treated RPMI8226 MM cells attracts γδT cells toward the injection port, providing further evidence that suggests that RPMI8226 MM cells secrete γδT cell chemotactic factors. It has been shown that the metabolite IPP accumulates in tumor cells following N-BP treatment, that it is recognized by γδT cells and that it is a potential chemoattractive factor [4], therefore we focused our investigation of chemotactic factors secreted from MM cells on IPP. The conventional migration assay, using a modified Boyden chamber, showed that IPP induced γδT cell migration in a dose-dependent manner. However, the possibility that γδT cells activated by IPP move randomly and migrate toward the lower chamber of the Boyden system is not excluded, whereas our μTAS-based microchamber clearly demonstrated the chemotaxis of γδT cells. Moreover, this microchamber enabled to observe that IPP also increased the speed of γδT cell migration significantly.

The fact that this μTAS-based microchamber has a very small volume (240 nL) and that the concentration gradient in the chamber is not influenced by fluid convection or stirring gives the

system two unique characteristics. Firstly, cell migration can be analyzed in a short period because of the minute chamber and microinjector [10]. Recently, Benzaïd et al. demonstrated that IPP induced γδT cell migration using a conventional transwell migration assay [17]. We confirmed the IPP-induced migration of γδT cells also in this study. The incubation times prior to evaluation of migration by Benzaïd and colleagues and in our transwell experiments are 24 and 4 h, respectively. However, using a microchamber, we could detect the migration of γδT cells only within 30 min. Moreover, this microchamber analysis revealed that IPP dramatically enhanced γδT cell migration compared with the analysis used the transwell chamber. The minute size of our chamber means that the profile of the concentration gradient within it remains more stable than in the conventional transwell chamber [10]. Moreover, our μTAS-based microchamber enables us to observe live cell image under a microscope [10]. Consequently, we were able to detect migration directly for 30 min and analyze their chemotaxis statistically in <100 cells. The second unique characteristic of this μTAS-based microchamber is its ability to mimic secretion of a humoral factor from the cell surface. A solute injected via a microinjector can spread in a diffusion-dependent manner; thus, microinjection of a humoral factor mimics its release from a cell's surface (Fig. 4). This microchamber is therefore able to mimic the microenvironment in the immediate vicinity of the introduced cells.

In conclusion, we have demonstrated the activation of γδT cell migration using a μTAS-based microchamber. IPP, the mevalonate metabolite increased by ZOL treatment, activates γδT cell migration. There have been many clinical studies and clinical trials of immunotherapy against cancers using γδT-cells, but the outcomes have not necessarily been satisfactory [21–23]. It is expected that the higher the effector cell to tumor cell (E:T) ratio, the greater the cytotoxic impact on the tumor; however, increasing the E:T ratio in the clinical setting has limits because of adverse effects. Our observations suggest that cancer cells treated ZOL secrete IPP, which leads to their death via γδT cell killing. In other words, the metabolite IPP induced by ZOL is a suicide factor. This limitation may be overcome if γδT-cells can be stimulated to reach target tumor tissues more locally.

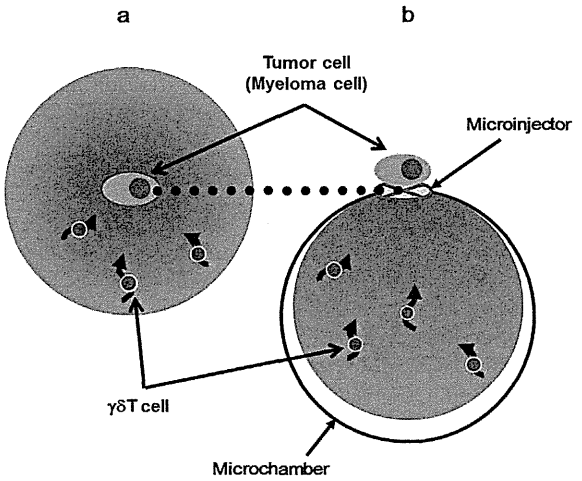

Fig. 4. Scheme of the μTAS-based microchamber mimicking the secretion of humoral factor released from the myeloma cell surface. (a) The secreted humoral factor spreads from the cell surface into the microenvironment in a diffusion-dependent manner. (b) The solute introduced via a microinjector can spread within the microchamber in a diffusion-dependent manner, mimicking the spread of humoral factor secreted from the myeloma cell surface. The gradient of color (gray) indicates that of the secreted humoral factor. γδT cells migrate in accordance with the gradient of the secreted humoral factor.

Conflict of interest statements

Conflict-of-interest disclosure: E. Ashihara, S. Kimura, Y. Nakagawa, H. Hirai, T. Miida, S. Yamato, S. Shoji, and Taira Maekawa disclose no financial conflict of interest. T. Munaka, M. Kanai, and H. Abe. are employees of Shimadzu Corporation.

Acknowledgments

This work was supported by a Grant-in-Aid from the Ministry of Education, Culture, Sports, Science and Technology (MEXT) in Japan (23591404, 26461436 to EA, 21591201 to SK, 24790175 to SN, 25461615, 11068019 to HH, and 23112507, 24390244, 25112706, 11068019 to TM). This work was also supported by Mitsubishi Pharma Medical Research Foundation (The 26th Grants for Basic Research of Hematology to EA), the Kobayashi Foundation for Cancer Research (The 6th Grants for Clinical Research of Oncology to TM), a Grant from Takeda Science Foundation (The Grants 2011 for Basic Research of Medical Scince to HH), and the Research Grant of the Princess Takamatsu Cancer Research Fund (13-24521 to TM).

Appendix A. Supplementary data

Supplementary data related to this article can be found at http://dx.doi.org/10.1016/j.bbrc.2015.05.118.

Transparency document

Transparency document related to this article can be found online at http://dx.doi.org/10.1016/j.bbrc.2015.05.118.

References

[1] K. Sato, S. Kimura, H. Segawa, A. Yokota, S. Matsumoto, J. Kuroda, M. Nogawa, T. Yuasa, Y. Kiyono, H. Wada, T. Maekawa, Cytotoxic effects of gammadelta T cells expanded ex vivo by a third generation bisphosphonate for cancer immunotherapy, Int. J. Cancer 116 (2005) 94–99.
[2] R. Uchida, E. Ashihara, K. Sato, S. Kimura, J. Kuroda, M. Takeuchi, E. Kawata, K. Taniguchi, M. Okamoto, K. Shimura, Y. Kiyono, C. Shimazaki, M. Taniwaki, T. Maekawa, Gamma delta T cells kill myeloma cells by sensing mevalonate metabolites and ICAM-1 molecules on cell surface, Biochem.. Biophys. Res. Commun. 354 (2007) 613–618.
[3] T. Yuasa, K. Sato, E. Ashihara, M. Takeuchi, S. Maita, N. Tsuchiya, T. Habuchi, T. Maekawa, S. Kimura, Intravesical administration of gammadelta T cells successfully prevents the growth of bladder cancer in the murine model, Cancer Immunol. Immunother. 58 (2009) 493–502.
[4] H.J. Gober, M. Kistowska, L. Angman, P. Jeno, L. Mori, G. De Libero, Human T cell receptor gammadelta cells recognize endogenous mevalonate metabolites in tumor cells, J. Exp. Med. 197 (2003) 163–168.
[5] H. Das, V. Groh, C. Kuijl, M. Sugita, C.T. Morita, T. Spies, J.F. Bukowski, MICA engagement by human Vgamma2Vdelta2 T cells enhances their antigen-dependent effector function, Immunity 15 (2001) 83–93.
[6] Y. Kato, Y. Tanaka, M. Hayashi, K. Okawa, N. Minato, Involvement of CD166 in the activation of human gamma delta T cells by tumor cells sensitized with nonpeptide antigens, J. Immunol. 177 (2006) 877–884.
[7] O. Toutirais, F. Cabillic, G. Le Friec, S. Salot, P. Loyer, M. Le Gallo, M. Desille, C.T. de La Pintiere, P. Daniel, F. Bouet, V. Catros, DNAX accessory molecule-1 (CD226) promotes human hepatocellular carcinoma cell lysis by Vgamma9Vdelta2 T cells, Eur. J. Immunol. 39 (2009) 1361–1368.
[8] S. Yamashita, Y. Tanaka, M. Harazaki, B. Mikami, N. Minato, Recognition mechanism of non-peptide antigens by human gammadelta T cells, Int. Immunol. 15 (2003) 1301–1307.
[9] B.J. Kim, M. Wu, Microfluidics for mammalian cell chemotaxis, Ann. Biomed. Eng. 40 (2012) 1316–1327.
[10] T.M. Keenan, A. Folch, Biomolecular gradients in cell culture systems, Lab. Chip 8 (2008) 34–57.
[11] M.L. Kovarik, P.C. Gach, D.M. Ornoff, Y. Wang, J. Balowski, L. Farrag, N.L. Allbritton, Micro total analysis systems for cell biology and biochemical assays, Anal. Chem. 84 (2012) 516–540.
[12] C.T. Culbertson, T.G. Mickleburgh, S.A. Stewart-James, K.A. Sellens, M. Pressnall, Micro total analysis systems: fundamental advances and biological applications, Anal. Chem. 86 (2014) 95–118.
[13] E.K. Sackmann, A.L. Fulton, D.J. Beebe, The present and future role of microfluidics in biomedical research, Nature 507 (2014) 181–189.

[14] T. Munaka, H. Abe, M. Kanai, T. Sakamoto, H. Nakanishi, S. Shoji, S. Kimura, T. Maekawa, A. Murakami, Real-time monitoring of antibody secretion from B-cells on a microchip stimulated with a minute amount of mitogen, Analyst 132 (2007) 512–514.
[15] M. Kanai, H. Abe, T. Munaka, Y. Fujiyama, D. Uchida, A. Yamayoshi, H. Nakanishi, A. Murakami, S. Shoji, Micro chamber for cellar analysis integrated with negligible dead volume sample injector, Sensors Actuators A: Phys. 114 (2004) 129–134.
[16] L. Henneman, A.G. van Cruchten, S.W. Denis, M.W. Amolins, A.T. Placzek, R.A. Gibbs, W. Kulik, H.R. Waterham, Detection of nonsterol isoprenoids by HPLC-MS/MS, Anal. Biochem. 383 (2008) 18–24.
[17] I. Benzaid, H. Monkkonen, V. Stresing, E. Bonnelye, J. Green, J. Monkkonen, J.L. Touraine, P. Clezardin, High phosphoantigen levels in bisphosphonate-treated human breast tumors promote Vgamma9Vdelta2 T-cell chemotaxis and cytotoxicity in vivo, Cancer. Res. 71 (2011) 4562–4572.
[18] V. Lafont, J. Liautard, M. Sable-Teychene, Y. Sainte-Marie, J. Favero, Isopentenyl pyrophosphate, a mycobacterial non-peptidic antigen, triggers delayed and highly sustained signaling in human gamma delta T lymphocytes without inducing eown-modulation of T cell antigen receptor, J. Biol. Chem. 276 (2001) 15961–15967.
[19] B. Rincon-Orozco, V. Kunzmann, P. Wrobel, D. Kabelitz, A. Steinle, T. Herrmann, Activation of V gamma 9V delta 2 T cells by NKG2D, J. Immunol. 175 (2005) 2144–2151.
[20] A.S. Idrees, T. Sugie, C. Inoue, K. Murata-Hirai, H. Okamura, C.T. Morita, N. Minato, M. Toi, Y. Tanaka, Comparison of gammadelta T cell responses and farnesyl diphosphate synthase inhibition in tumor cells pretreated with zoledronic acid, Cancer Sci. 104 (2013) 536–542.
[21] Y. Abe, M. Muto, M. Nieda, Y. Nakagawa, A. Nicol, T. Kaneko, S. Goto, K. Yokokawa, K. Suzuki, Clinical and immunological evaluation of zoledronate-activated Vgamma9gammadelta T-cell-based immunotherapy for patients with multiple myeloma, Exp. Hematol. 37 (2009) 956–968.
[22] J. Nakajima, T. Murakawa, T. Fukami, S. Goto, T. Kaneko, Y. Yoshida, S. Takamoto, K. Kakimi, A phase I study of adoptive immunotherapy for recurrent non-small-cell lung cancer patients with autologous gammadelta T cells, Eur. J. Cardiothorac. Surg. 37 (2010) 1191–1197.
[23] A.J. Nicol, H. Tokuyama, S.R. Mattarollo, T. Hagi, K. Suzuki, K. Yokokawa, M. Nieda, Clinical evaluation of autologous gamma delta T cell-based immunotherapy for metastatic solid tumours, Br. J. Cancer 105 (2011) 778–786.

Prevalence, Clinical Features, and Prognosis of Acute Myocardial Infarction Attributable to Coronary Artery Embolism

Tatsuhiro Shibata, MD; Shoji Kawakami, MD; Teruo Noguchi, MD; Tomotaka Tanaka, MD; Yasuhide Asaumi, MD; Tomoaki Kanaya, MD; Toshiyuki Nagai, MD; Kazuhiro Nakao, MD; Masashi Fujino, MD; Kazuyuki Nagatsuka, MD; Hatsue Ishibashi-Ueda, MD; Kunihiro Nishimura, MD; Yoshihiro Miyamoto, MD; Kengo Kusano, MD; Toshihisa Anzai, MD; Yoichi Goto, MD; Hisao Ogawa, MD; Satoshi Yasuda, MD

Background—Coronary artery embolism (CE) is recognized as an important nonatherosclerotic cause of acute myocardial infarction. Its prevalence, clinical features, and prognosis remain insufficiently characterized.

Methods and Results—We screened 1776 consecutive patients who presented with de novo acute myocardial infarction between 2001 and 2013. CE was diagnosed based on criteria encompassing histological, angiographic, and other diagnostic imaging findings. The prevalence, clinical characteristics, treatment strategies, in-hospital outcomes, and long-term risk of CE recurrence or major adverse cardiac and cerebrovascular events (cardiac death, fatal arrhythmia, or recurrent thromboembolism) were evaluated. The prevalence of CE was 2.9% (n=52), including 8 (15%) patients with multivessel CE. Atrial fibrillation was the most common cause (n=38, 73%). Only 39% of patients with CE were treated with vitamin K antagonists, and the median international normalized ratio was 1.42 (range, 0.95–1.80). Eighteen of the 30 CE patients with nonvalvular atrial fibrillation had a $CHADS_2$ score of 0 or 1. When those patients were reevaluated using CHA_2DS_2-VASc, 61% were reassigned to a higher risk category. During a median follow-up of 49 months, CE and thromboembolism recurred in 5 atrial fibrillation patients. The 5-year rate of major adverse cardiac and cerebrovascular events was 27.1%. In the propensity score–matched cohorts (n=45 each), Kaplan–Meier analysis showed a significantly higher incidence of cardiac death in the CE group than in the non-CE group (hazard ratio, 9.29; 95% confidence interval, 1.13–76.5; $P<0.001$).

Conclusions—Atrial fibrillation is the most frequent cause of CE. Patients with CE represent a high-risk subgroup of patients with acute myocardial infarction and require close follow-up. **(*Circulation*. 2015;132:241-250. DOI: 10.1161/CIRCULATIONAHA.114.015134.)**

Key Words: acute myocardial infarction ■ atrial fibrillation ■ coronary artery ■ embolism

Coronary artery embolism (CE) is recognized as an important nonatherosclerotic cause of acute myocardial infarction (AMI). However, the prevalence of this nonatherosclerotic entity remains unknown because it is difficult to diagnose in the acute setting. In a previous study based on autopsy or coronary angiography findings, 4% to 7% of AMI patients did not have atherosclerotic coronary disease.[1] In another autopsy study, 55 of 419 patients (13%) had coronary artery embolic infarcts.[2] In the era of primary percutaneous coronary intervention (PCI) for AMI, thrombectomy devices are increasingly used and histological examination of the aspirated thrombus provides additional information for diagnosing CE.[3] Because the majority of previous reports describing the clinical characteristics of CE were case reports with a small number of patients,[3–15] with the largest series to date consisting of 55 patients in an autopsy study[2] and 14 patients with probable CE in the clinical setting,[16] a mechanistic study for this important cause of AMI is now warranted.

Editorial see p 223
Clinical Perspective on p 250

Atrial fibrillation (AF) is associated with a high risk of thromboembolic events, and its prevalence is projected to increase because of population aging.[17] Indeed, the thromboembolic complications of AF are an important cause of morbidity and mortality. The $CHADS_2$ and CHA_2DS_2-VASc scores are useful for thromboembolic risk stratification.[18,19]

Continuing medical education (CME) credit is available for this article. Go to http://cme.ahajournals.org to take the quiz.
Received December 25, 2014; accepted May 15, 2015.

From Departments of Cardiovascular Medicine (T.S., S.K., T. Noguchi, Y.A., T.K., T. Nagai, K. Nakao, M.F., K.K., T.A., Y.G., H.O., S.Y.), Stroke and Cerebrovascular Disease (T.T., K. Nagatsuka), Pathology (H.I.-U.), and Preventive Medicine and Epidemiologic Informatics, Center for Cerebral and Cardiovascular Disease Information (K. Nishimura, Y.M.), National Cerebral and Cardiovascular Center, Suita, Japan.

The online-only Data Supplement is available with this article at http://circ.ahajournals.org/lookup/suppl/doi:10.1161/CIRCULATIONAHA.114.015134/-/DC1.

Correspondence to Teruo Noguchi, MD, PhD, Department of Cardiovascular Medicine, National Cerebral and Cardiovascular Center, 5-7-1 Fujishiro-dai, Suita, 565-8565, Japan. E-mail tnoguchi@hsp.ncvc.go.jp

Circulation **is available at http://circ.ahajournals.org** **DOI: 10.1161/CIRCULATIONAHA.114.015134**